  Bull. Chem. Soc. Jpn., 53, 975—979 (1980)

Spin Exchange and Translational Diffusion of Nitroxide Radicals in Micelles. ESR Experiments and Spectra Simulation by Modified Bloch Equations

Masayuki AIZAWA,* Tsuyoshi KOMATSU, and Tsurutaro NAKAGAWA
Department of Polymer Science, Faculty of Science, Hokkaido University, Sapporo 060
(Received August 6, 1979)

The dependence of the ESR linewidth of hydrophobic radicals on their concentration in micelles is investigated in two solubilization systems at several temperatures. One system consists of 2,2,6,6-tetramethyl-4-benzoyloxy-1-piperidinyloxyl (BzONO) as a solubilizate and hexadecyltrimethylammonium bromide (CTAB) as a surfactant, and the other, of 2,2,6,6-tetramethyl-4-myristoyloxy-1-piperidinyloxyl (MyONO) and sodium dodecyl sulfate (SDS). The plot of the linewidth against the mole fraction of the radical is not represented by a straight line, as in the previous study. The propriety of the two kinds of models for the solubilization states of radicals which were proposed in the previous paper to explain the unusual shape of these plots is examined by spectra simulation with modified Bloch equations. As these models have proved to be inadequate, a new model taking account of the distribution of the radicals among the micelles is proposed. The simulation based on this model shows a good agreement with the experimental results. The translational diffusion coefficients of radicals in micelles are estimated on the basis of this model. Their values are in the range of $(1.5—2.9)\times10^{-11}$ m²/s.

In the previous study,[1] linewidth measurements of the ESR spectra of 2,2,6,6-tetramethyl-4-benzoyloxy-1-piperidinyloxyl (BzONO, Fig. 1(a)) in sodium dodecyl sulfate (SDS) micelles were carried out at various concentrations of BzONO. The plot of the linewidth, W, against the mole fraction, X, of the radical in micelles did not yield a straight line; rather, a break point seemingly appeared at a certain mole fraction, X_B. Except for one other workers' study,[2] no results like this have yet been reported.

Considering the electron spin-spin relaxation mechanism which causes the line broadening, it was inferred that the dipolar interaction predominates at $X<X_B$, whereas the spin-exchange interaction predominates at $X\geqq X_B$. This inference is based on the temperature dependence of the gradients of the lines in the two mole fraction ranges: at $X<X_B$, the gradient decreases with an increase in the temperature, but at $X\geqq X_B$, it behaves inversely.

In order to explain these unusual results, three kinds of models for a solubilization state of radicals were proposed. From the two of them, the translational diffusion coefficients of BzONO in SDS micelles at 31 °C were estimated to be 1.6×10^{-11} and 2.4×10^{-11} m²/s respectively.

Recently, studies of micellar solutions have been carried out with fluorescent probes.[3] The measurements of the fluorescence decay or quenching, the excimer formation, and so on have brought out several interesting pieces of information on micellar properties.

Some abnormal results, however, have been reported by these studies. For instance, Khuanga and his coworkers[4] have found that the concentration dependence of the intensity ratio ϕ'/ϕ of excimer/monomer fluorescence of pyrene in a 0.1 M aqueous SDS solution is not linear, but curves upwards at higher concentrations, and that when the quencher, oxygen, is added to the solution, the ϕ'/ϕ is increased. In homogeneous solutions, however, the addition of quenchers never increases ϕ'/ϕ. They have explained these results qualitatively on the basis of the distribution of the pyrene molecules among the micelles.

The unusual results obtained in our previous study may also be explained on the same basis.

Thus, the purposes of the present study are: a) to assure that other solubilization systems give a similar, unusual behavior of the W-X plots; b) to reexamine the propriety of the three models in the previous paper; c) to examine whether or not the behavior of the W-X plots can be explained by the distribution of the solubilizates among the micelles, and, finally, d) to estimate more reasonably the translational diffusion coefficients of the radicals in the surfactant micelles.

In order to achieve b) and c), the experimental spectra will be simulated by modified Bloch equations, including the terms for two exchange processes: spin exchange in the micelles and exchange of radicals between the bulk water and the micellar environment.

Experimental

The nitroxide radical, 2,2,6,6-tetramethyl-4-myristoyloxy-1-piperidinyloxyl (MyONO, Fig. 1(b)), was synthesized by the reaction of the corresponding acid chloride with the nitroxide alcohol in a way similar to that in the literature.[5] The crude MyONO was purified by Mr. Fujioka by column chromatography with silica gel (CH_2Cl_2 as the eluent), and then distilled at 122—124 °C under 1 mmHg. The results of the elemental analysis of MyONO was as follows: Found: C, 72.41; H, 11.71; N, 3.43%. Calcd for $C_{23}H_{44}NO_3$: C, 72.20; H, 11.59; N, 3.66%; mol wt 382.6.

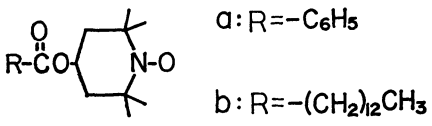

Fig. 1. (a) BzONO and (b) MyONO.

Hexadecyltrimethylammonium bromide (CTAB) of an extra pure grade was recrystallized several times from water solutions. Its CMC was 9.2×10^{-4} mol/dm³ at 25 °C.

In order to estimate the solubilization limits of radicals in surfactant solutions, the ESR spectra of radicals in the saturated solutions were recorded at 20, 30, and 40 °C.

The calculation of the spectra simulation was executed by means of the FACOM 230-60/75 computer in the Hokkaido University Computing Center.

The other experimental procedures and materials have been described in previous papers.[1,6]

Results and Discussion

As an example of the homogeneous solutions, the *W-X* plot of BzONO in ethanol is shown in Fig. 2. The linear relationship between W and X in the figure agrees with the theory of spin-spin interaction in homogeneous solutions.[7]

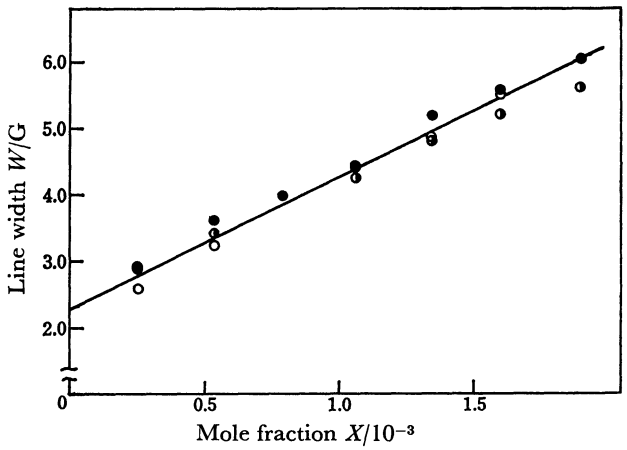

Fig. 2. Plot of W against X of BzONO in ethanol solution at 21 °C. ○: $M_I=+1$, ◑: $M_I=0$, and ●: $M_I=-1$ line width.

In SDS micelles in water, however, the same plot gives a straight line with a break point, as was reported in a previous paper.[1]

In the present study, two solubilization systems, BzONO/CTAB and MyONO/SDS, are investigated at several temperatures in a similar way.

Figures 3 and 4 show the *W-X* plots of MyONO/SDS at 30 °C and of BzONO/CTAB at 40 °C respectively. It may be observed that there is no simple linear relationship between W and X such as is seen in Fig. 2. The plots of the other results showed similar behavior.

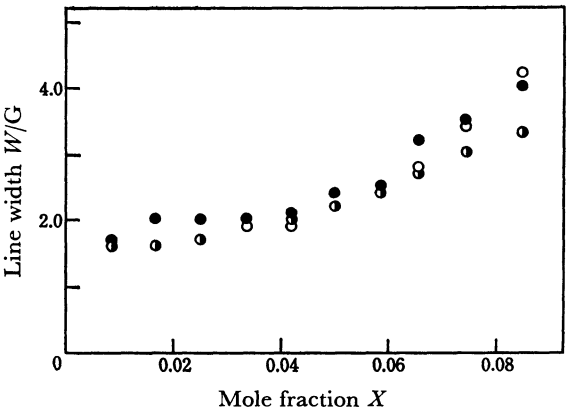

Fig. 3. Plot of W against X of MyONO in SDS micelles at 30 °C. ○: $M_I=+1$, ◑: $M_I=0$, and ●: $M_I=-1$ line width. [SDS]=5.30 wt%.

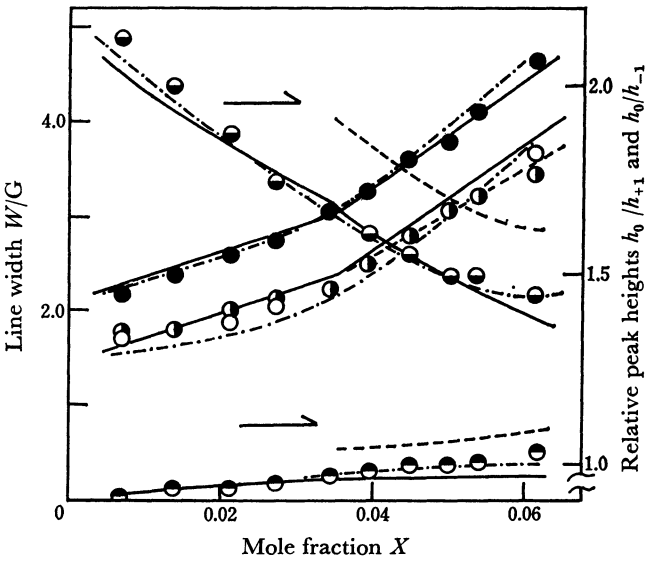

Fig. 4. Plots of W, h_0/h_{+1}, and h_0/h_{-1} against X of BzONO in CTAB micelles at 40 °C.
○: $M_I=+1$, ◑: $M_I=0$, and ●: $M_I=-1$ line width; ◓: h_0/h_{+1} and ◒: h_0/h_{-1}. [CTAB]=5.12%. Full, dotted and dot-dash lines represent the same plots obtained by the simulation with Model 1, Model 2, and the new model in which the distribution of solubilizates among micelles is considered, respectively.

If one considers that the plots can be represented by a straight line which breaks at a certain mole fraction, X_B, the value of X_B is estimated to be 0.035 for BzONO/CTAB and 0.045 for MyONO/SDS. The latter value coincides with that for BzONO/SDS.[1]

Thus, it may be concluded that, in the cases of radicals in ionic micelles in water, the concentration dependence of the linewidth is different from that in homogeneous solutions.

In the previous paper,[1] in seeking to explain this behavior of the *W-X* plots, three kinds of models for the solubilization states of the radicals in the micelles were proposed; they could account for, at least, the appearance of a break point. The propriety of the models, however, must also be examined by spectra simulation with modified Bloch equations.[8]

In the present solubilization systems, most of the nitroxide radicals are solubilized in a micellar environment, while a small amount of them is dissolved in the bulk water. In each of the two environments, the radicals exist in three energy states, which are split by the contact interaction between an electron spin ($S=1/2$) and a ^{14}N nuclear spin ($I=1$). Between the six energy states, there are two exchange processes: one is the exchange of a radical between the micellar environment and the bulk water,[9] and the other is a spin exchange in the micellar environment.[10] The spin exchange in the bulk water can be disregarded, since a molecular collision between radicals scarcely occurs in it at all.

Thus, the exchange scheme in the system is illustrated by Fig. 5. The symbols in the figure, W_{-1}, W_0, and W_{+1}, represent the three states in the bulk water, and M_{-1}, M_0, and M_{+1}, those in the micellar environment.

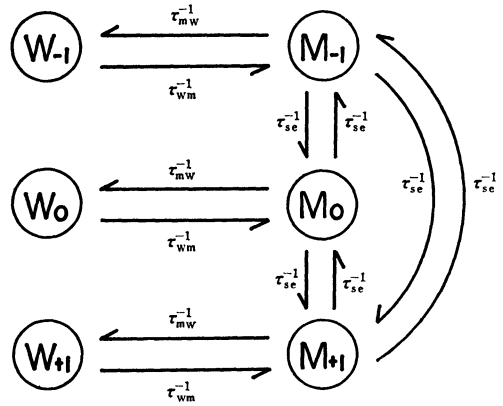

Fig. 5. Proposed scheme of radical exchange.

Their subscripts, -1, 0, and $+1$, correspond to the quantum numbers of a ^{14}N nuclear spin. τ_{mw}^{-1}, τ_{wm}^{-1}, and τ_{se}^{-1} are the exchange probabilities in the corresponding processes.

The modified Bloch equations including these exchange processes are formulated as follows:

$$\begin{cases} dG_{-1}^{w}/dt + \alpha_{-1}^{w}G_{-1}^{w} = Lp_{-1}^{w} - \tau_{wm}^{-1}G_{-1}^{w} + \tau_{mw}^{-1}G_{-1}^{m} \\ dG_{0}^{w}/dt + \alpha_{0}^{w}G_{0}^{w} = Lp_{0}^{w} - \tau_{wm}^{-1}G_{0}^{w} + \tau_{mw}^{-1}G_{0}^{m} \\ dG_{+1}^{w}/dt + \alpha_{+1}^{w}G_{+1}^{w} = Lp_{+1}^{w} - \tau_{wm}^{-1}G_{+1}^{w} + \tau_{mw}^{-1}G_{+1}^{m} \\ dG_{-1}^{m}/dt + \alpha_{-1}^{m}G_{-1}^{m} = Lp_{-1}^{m} + \tau_{wm}^{-1}G_{-1}^{w} - \tau_{mw}^{-1}G_{-1}^{m} \\ \qquad + \tau_{se}^{-1}(G_{+1}^{m}+G_{0}^{m}) - 2\tau_{se}^{-1}G_{-1}^{m} \\ dG_{0}^{m}/dt + \alpha_{0}^{m}G_{0}^{m} = Lp_{0}^{m} + \tau_{wm}^{-1}G_{0}^{w} - \tau_{mw}^{-1}G_{0}^{m} \\ \qquad + \tau_{se}^{-1}(G_{-1}^{m}+G_{+1}^{m}) - 2\tau_{se}^{-1}G_{0}^{m} \\ dG_{+1}^{m}/dt + \alpha_{+1}^{m}G_{+1}^{m} = Lp_{+1}^{m} + \tau_{wm}^{-1}G_{+1}^{w} - \tau_{mw}^{-1}G_{+1}^{m} \\ \qquad + \tau_{se}^{-1}(G_{0}^{m}+G_{-1}^{m}) - 2\tau_{se}^{-1}G_{+1}^{m} \end{cases} \quad (1)$$

where:

$$\alpha_{-1}^{w} = T_{2w}^{-1}(-1) + i(H-H_{-1}^{w}),$$
$$\alpha_{-1}^{m} = T_{2m}^{-1}(-1) + i(H-H_{-1}^{m}),$$
$$\alpha_{0}^{w} = T_{2w}^{-1}(0) + i(H-H_{0}^{w}),$$
$$\alpha_{0}^{m} = T_{2m}^{-1}(0) + i(H-H_{0}^{m}),$$
$$\alpha_{+1}^{w} = T_{2w}^{-1}(+1) + i(H-H_{+1}^{w}),$$
$$\alpha_{+1}^{m} = T_{2m}^{-1}(+1) + i(H-H_{+1}^{m}),$$

and $L=-2\pi i\nu M_0=$constant.

The notations in these equations have the following meanings.

G_{-1}^{w}, G_{0}^{w}, G_{+1}^{w}, and G_{-1}^{m}, G_{0}^{m}, G_{+1}^{m}: the complex magnetic moments at the energy states, with $M_I=-1$, 0, $+1$ in the bulk water, and with $M_I=-1$, 0, $+1$ in the micellar environment respectively.

$T_{2w}^{-1}(-1)$, $T_{2w}^{-1}(0)$, $T_{2w}^{-1}(+1)$, and $T_{2m}^{-1}(-1)$, $T_{2m}^{-1}(0)$, $T_{2m}^{-1}(+1)$: the spin-spin relaxation rates in the energy states, with $M_I=-1$, 0, $+1$ in the bulk water, and with $M_I=-1$, 0, $+1$ in the micellar environment respectively.

p_{-1}^{w}, p_{0}^{w}, p_{+1}^{w}, and p_{-1}^{m}, p_{0}^{m}, p_{+1}^{m}: the mole fractions of the radicals in the energy states, with $M_I=-1$, 0, $+1$ in the bulk water, and with $M_I=-1$, 0, $+1$ in the micellar environment respectively. $p_{-1}^{w}=p_{0}^{w}=p_{+1}^{w}=(1/3)p_w$, $p_{-1}^{m}=p_{0}^{m}=p_{+1}^{m}=(1/3)p_m$.

H_{-1}^{w}, H_{0}^{w}, H_{+1}^{w}, and H_{-1}^{m}, H_{0}^{m}, H_{+1}^{m}: the strength of the resonance magnetic fields in the energy states, with $M_I=-1$, 0, $+1$ in the bulk water, and with $M_I=-1$, 0, $+1$ in the micellar environment respectively. $H_{-1}^{w}-H_{0}^{w}=H_{0}^{w}-H_{+1}^{w}$, $H_{-1}^{m}-H_{0}^{m}=H_{0}^{m}-H_{+1}^{m}$.

ν: the frequency of the applied rotating *rf* field.

M_0: the z-component of the equilibrium magnetic moment.

i: the imaginary unit.

The sum of the solutions of these equations under the condition that $dG_{-1}^{w}/dt=\cdots=dG_{+1}^{m}/dt=0$ gives the total complex magnetic moment, G, in the stationary state. The real part of G corresponds to the dispersion line, and the imaginary part, to the absorption. Since the first derivative of the absorption line is recorded in the ESR experiment, the first derivative of G is obtained; its imaginary part, $f(H)$, is calculated for the sake of the spectra simulation as a function of the strength of the magnetic field, H—in practice, as a function of $(H-H_0^w)$.

Among the input values needed for the calculation of $f(H)$, τ_{mw}^{-1}, τ_{se}^{-1}, and the mole fraction, p_m, of the radicals in the micelles are fitting parameters, since $p_w=1-p_m$ and $\tau_{wm}^{-1}=\tau_{mw}^{-1}p_m/p_w$ hold. In the present systems, p_m is nearly equal to 1.0 and τ_{mw}^{-1} is negligibly small, as was reported in previous papers.[11,12]

Moreover, the spin-spin relaxation rate, T_{2D}^{-1}, by the dipolar interaction must be introduced as a parameter, since, in all three models, the dipolar interaction is considered to be an electron spin-spin interaction as well as a spin-exchange interaction. T_{2D}^{-1} is added to the spin-spin relaxation rates, T_{2m}^{-1}'s, in the micelles.

The other input values are obtained from the ESR spectra at a low radical concentration in water and from those in micelles. The values of T_{2m}^{-1}'s, however, are corrected to fit the experimental values of the relative peak heights of the three lines. This is because the linewidth, $W(=(2/\sqrt{3})T_2^{-1})$, in the present systems contains a contribution from the protons in the methyl groups adjacent to a nitroxide group in addition to that from a ^{14}N nuclear spin.[13] Equation 1 includes only the effect of a ^{14}N nuclear spin.

The concentration dependences of T_{2D}^{-1} and τ_{se}^{-1} as parameters will now be described on the basis of the respective models.

Model 1. According to this model, a micelle is constituted of several clusters of some surfactant molecules. Therefore, below the break point, X_B, which corresponds to the concentration at which each cluster solubilizes just one radical, only the dipolar interaction occurs.

On the other hand, above X_B, the spin-exchange interaction relaxes the electron spins as well as the dipolar interaction.

Thus, T_{2D}^{-1} and τ_{se}^{-1} can be written, at $X<X_B$, as:

$$\begin{cases} T_{2D}^{-1} = K_D X \\ \tau_{se}^{-1} = 0, \end{cases} \quad (2\text{-a})$$

and at $X\geqq X_B$, as:

$$\begin{cases} T_{2D}^{-1} = K_D X \\ \tau_{se}^{-1} = k_E'(X-X_B), \end{cases} \quad (2\text{-b})$$

where K_D and k_E' are the proportionality constants.

Model 2. In this model, X_B is regarded as the concentration at which a structural change in the micelles is induced by the solubilization. This structural

change quickly makes the dipolar interaction weaker near X_B.

T_{2D}^{-1} and τ_{se}^{-1} are given by the following expressions: At $X<X_B$;

$$\begin{cases} T_{2D}^{-1} = K_D X \\ \tau_{se}^{-1} = 0. \end{cases} \quad (3\text{-a})$$

At $X \geqq X_B$;

$$\begin{cases} T_{2D}^{-1} = 0 \\ \tau_{se}^{-1} = k'_E X. \end{cases} \quad (3\text{-b})$$

Model 3. This model, in which some association of the radicals in equilibrium with the monomeric one in a micelle is assumed, cannot be employed in the simulation, because it is impossible to separate the signal of the radical associates from that of monomeric ones. This fact indicates that this model is not applicable to the solubilization state of radicals.

Thus, on the first two models, the simulation was carried out by the calculation of $f(H)$ using the values of $p_m=1.0$ and $\tau_{mw}^{-1}=0$ and the parameters of τ_{se}^{-1} and T_{2D}^{-1}. The values of parameters which fit the experimental linewidth and the relative peak height were thus found.

The full lines and dotted lines in Fig. 4 represent the results of the simulations with Model 1 and Model 2 respectively. The relative peak heights, h_0/h_{+1} and h_0/h_{-1}, indicate the ratios of the peak height of the central line ($M_I=0$) to that of the low- ($M_I=+1$) and high-field ($M_I=-1$) lines respectively.

The full lines with $K_D=20.1$ G ($=2.01\times10^{-3}$ T) and $k'_E=15.6$ G and the dotted ones with $K_D=20.1$ G and $k'_E=25.7$ G agree with the experimental values so far as the linewidth is concerned. There is, however, a difference in the relative peak heights. The experimental values of h_0/h_{-1} decrease monotonously throughout the mole-fraction range, while the full line has a discontinuity of its gradient at X_B and does not agree with the experimental values at lower and higher mole fractions. The dotted line also has a discontinuity at X_B. (At $X<X_B$, the dotted lines coincide with the full ones).

Therefore, it can be said that each of the three models proposed in the previous study is improper as a basis for the calculation of the translational diffusion coefficients of the radicals in the micelles.

Another way to explain the unusual W-X plot is by taking account of the distribution of the radicals among the micelles. If one regards a micelle as a thermodynamical system which is surrounded by an aqueous phase and which is exchanging its components with the aqueous phase, there may be a certain distribution in the number of the radicals among the micelles.

The distribution function, $P_m(n)$, is described by the following equation, known as the binomial function:[14]

$$P_m(n) = {}_{N_m}C_n \chi^n/(1+\chi)^{N_m}, \quad (4)$$

$$\chi = \langle n\rangle/(N_m-\langle n\rangle), \quad (5)$$

where ${}_{N_m}C_n$ is the binomial coefficient; N_m, the maximum number of solubilizates in a micelle; χ, the quantity defined by Eq. 5 and related with the chemical potential of solubilizates in micelles, and $\langle n\rangle$, the mean number of solubilizates in a micelle.

$P_m(n)$ indicates the fraction of the number of micelles with n solubilizates in relation to the total micelles. This function is obtained on the assumptions that χ is independent of n and that all the micelles have the same N_m value. If $n \ll N_m$, the Poisson distribution function can be derived from Eq. 4.

Transforming $P_m(n)$ into the probability, $P_r(n)$, that a solubilizate belongs to a micelle with n solubilizates, one can write:

$$P_r(n) = nP_m(n)/\sum_{n=1}^{N_m} nP_m(n). \quad (6)$$

If the line-shape function, $f_n(H)$, of a radical in a micelle with n radicals is given, the apparent line-shape function, $F(H)$, is calculated as:

$$F(H) = \sum_{n=1}^{N_m} P_r(n) f_n(H). \quad (7)$$

Thus, the spectra simulation on this model is carried out as follows.

Firstly, $f_n(H)$ is calculated using four parameters, p_m, τ_{se}^{-1}, τ_{mw}^{-1}, and T_{2D}^{-1}, in the same way as in the previous case of $f(H)$. τ_{mw}^{-1}, however, can be neglected for the above-mentioned reason. T_{2D}^{-1} is also omitted, since the radicals in the micelles have enough mobility to make the dipolar interaction fade away, according to Scandella and his co-workers' results.[15]

The spin-exchange rate, τ_{se}^{-1} in a micelle with n radicals is described as:

$$\tau_{se}^{-1} = K_s(n-1)(N_s+1)/(N_s+n-1), \quad (8)$$

where K_s is constant and corresponds to τ_{se}^{-1} when $n=2$, and where N_s is the aggregation number of the surfactant molecules in a micelle. Here, as N_s, the mean aggregation number given in the literature[3] is used in the case of CTAB. However, in the SDS system, one is obliged to use a value lower than that in the literature, since the value in the literature produces the break point at a mole fraction lower than the experimental one. As p_m in Eq. 1, values near 1.0 are used.

TABLE 1. INPUT VALUES USED IN SPECTRA SIMULATION

	a_N^w/G	a_N^m/G	Δg_{mw}/G	N_s	N_m
BzONO/SDS	17.1	16.7	0.2	54	7
MyONO/SDS	17.1	16.6	0.2	54 (44)[a]	11 (9)[a]
BzONO/CTAB	17.1	16.3	0.4	60	6

a) The values at 40 °C.

These values and other input values are listed in Table 1. $a_N^w(=(H_{-1}^w-H_{+1}^w)/2)$ and $a_N^m(=(H_{-1}^m-H_{+1}^m)/2)$, respectively, mean the isotropic hyperfine splitting constants of the radicals in the bulk water and in the micellar environment. Δg_{mw} represents the difference in the resonance magnetic field of the central line between the two environments, $H_0^w-H_0^m$.

Secondly, using arbitrary values of $\langle n\rangle$ lower than N_m, $P_m(n)$ is calculated by means of Eqs. 4 and 5, and then $P_r(n)$ is derived from Eq. 6. Here, N_m is obtained from a mole fraction of a radical saturated in a micelle. The estimation of its mole fraction is performed by plotting the linewidth of the ESR spectra of the radicals

TABLE 2. K_s VALUES AND TRANSLATIONAL DIFFUSION COEFFICIENTS OF NITROXIDE RADICALS IN MICELLES

Temp °C	BzONO/SDS		MyONO/SDS		BzONO/CTAB	
	K_s/G	$D_{tr}/10^{-11}$ m^2 s^{-1}	K_s/G	$D_{tr}/10^{-11}$ m^2 s^{-1}	K_s/G	$D_{tr}/10^{-11}$ m^2 s^{-1}
20	0.40—0.45	1.8—2.0	0.33—0.35	1.5—1.6		
30	0.53—0.58[a)]	2.4—2.6[a)]	0.38—0.43	1.7—1.9	0.35—0.38	1.9—2.0
40	0.60—0.65	2.7—2.9	0.60—0.63	2.2—2.3	0.40—0.45	2.1—2.4
50					0.45—0.50	2.4—2.7

a) The values at 31°C.

saturated in the micellar solution on the W-X curves.

Finally, by substituting these $f_n(H)$ and $P_r(n)$ into Eq. 7, the apparent line-shape function, $F(H)$, at $<n>$ is obtained. If one executes a similar calculation of $F(H)$ with various values of $<n>$, the W-X plot can be represented by this relation: $<n>=Xp_mN_s/(1-X)$.

The dot-dash lines in Fig. 4 show the results of simulation on BzONO/CTAB at 40 °C by the calculation of $F(H)$. These lines were obtained by the simulation with $p_m=0.98$ and $K_s=0.45$ G. It may be observed that the dot-dash lines are in good agreement with the experimental values.

Therefore, it may be said that the appearance of an apparent break point in the W-X plot is caused by the distribution of the radicals among the micelles. The relation that the peak heights are inversely proportional to the square of their linewidths in the spectra of the Lorentzian lineshape contributes greatly to the phenomenon.

All the other systems are also simulated very well by this scheme. The values of K_s which give the best fits are listed in Table 2.

The translational diffusion coefficients, D_{tr}, of the nitroxide radicals in the micelles were calculated with the following equation, using these K_s values:

$$D_{tr} = \gamma_e K_s \lambda^2 (1+N_s)/4\pi \quad (9)$$

where $\gamma_e(=1.7608\times10^7$ s/rad·G) is the magnetogyric ratio of the electron and where λ^2 is the surface area of one polar head group. The values of λ^2 in the SDS micelles and the CTAB micelles are 5.8×10^{-15} and 6.2×10^{-15} cm^2 respectively.[16] Strictly speaking, the effects of the difference in the solubilization site of the solubilizates and of the deformation of the micellar shape induced by the solubilization of the radicals must also be taken into account in Eq. 9.

The values of D_{tr} obtained are listed in Table 2. These values are of the order of 10^{-11} m^2/s, the same as in the previous study.[1] They are taken to be reliable enough, because they are calculated on a reasonable model, as has been revealed in the above simulation.

It may be noticed in Table 2 that, at the same temperature, D_{tr} in BzONO/SDS is greater than in either MyONO/SDS or BzONO/CTAB. This fact may be related to the strength of the adhesion between the hydrophobic groups of the radicals and those of the surfactant molecules.

We would like to thank Professor Yoshio Matsunaga of the Department of Chemistry in Hokkaido University for his kind permission to use the ESR instruments.

References

1) M. Aizawa, T. Komatsu, and T. Nakagawa, *Bull. Chem. Soc. Jpn.*, **52**, 980 (1979).
2) M. D. Barrat, F. Franks, and P. N. Robinson, *J. Solution Chem.*, **6**, 625 (1977).
3) J. H. Fendler and E. J. Fendler, "Catalysis in Micellar and Macromolecular Systems," Academic Press, New York, N. Y. (1975), pp. 20, 293—301.
4) U Khuanga, B. K. Selinger, and R. McDonald, *Aust. J. Chem.*, **29**, 1 (1976).
5) E. G. Rozantsev and V. A. Golubev, *Izv. Akad. Nauk SSSR, Ser. Khim.*, **1968**, 1191.
6) M. Aizawa, T. Komatsu, and T. Nakagawa, *Bull. Chem. Soc. Jpn.*, **50**, 3107 (1977).
7) Y. Ayant, R. Besson, and A. Salvi, *J. Phys. (Paris)*, **36**, 571 (1975).
8) A. Carrington and A. D. McLachlan, "Introduction to Magnetic Resonance," Harper and Row, New York, N. Y. (1967), pp. 204—208.
9) T. Nakagawa and H. Jizomoto, *Kolloid Z.Z. Polym.*, **250**, 594 (1972).
10) E. Odgard, T. B. Melø, and T. Henriksen, *J. Magn. Reson.*, **18**, 436 (1975).
11) G. Aniasson, S. Wall, M. Almgren, H. Hoffman, I. Kielman, W. Ulbricht, R. Zana, J. Lang, and C. Tondre, *J. Phys. Chem.*, **80**, 905 (1976).
12) T. Nakagawa, *Colloid Polym. Sci.*, **252**, 56 (1974).
13) A. E. Stillman and R. N. Schwartz, *J. Magn. Reson.*, **22**, 269 (1976).
14) C. Kittel, "Thermal Physics," John Wiley and Sons, New York, N. Y. (1969), pp. 395—402.
15) C. J. Scandella, P. Devaux, and H. M. McConnell, *Proc. Natl. Acad. Sci. U. S. A.*, **69**, 2056 (1972).
16) H. V. Tartar, *J. Phys. Chem.*, **59**, 1195 (1955).